J. Jpn. Soc. Soil Phys.
土壌の物理性
No. 157 p.19 ～ 32 (2024)

若手特集
論　文
Original Paper

Estimating soil hydraulic and thermal properties using publicly available soil information for future prediction of soil temperature and water content

Juri ASANO[1], Yuki KOJIMA[2], Chihiro KATO[3] and Kohji KAMIYA[2]

Abstract: Determining the soil hydraulic and thermal properties is necessary for predicting the future soil temperature and water content. However, it requires a long time, enormous effort, and considerable expense, including soil sampling from the target site, laboratory testing, and optimization processing based on field observations. This study estimated soil hydraulic and thermal properties using publicly available soil information and pedotransfer functions, and examined their usefulness. Soil information was extracted from the Japanese Soil Inventory, and several pedotransfer functions were tested. The results of soil temperature and water content computations using the estimated soil hydraulic and thermal properties were compared with the computations using soil hydraulic and thermal properties obtained from previous studies. The estimation approach that minimized the error between the two was selected as the optimal approach. Then, the future soil temperature and water content were computed using the soil hydraulic and thermal properties obtained by the optimal estimation approach and compared with the results of previous studies. The predictions of volumetric water content and soil temperature differed due to the estimated soil hydraulic and thermal properties, but there was no significant difference in the magnitude of change between the present and future. This indicates that estimating soil hydraulic and thermal properties using publicly available soil information and pedotransfer functions may be acceptable if the estimation is limited to evaluating future changes.
Key Words : pedotransfer function, soil hydraulic properties, soil thermal properties, climate change, HYDRUS-1D

1. Introduction

In recent years, climate change due to global warming has caused changes in temperature, precipitation, and precipitation patterns. The Intergovernmental Panel on Climate Change (IPCC) Sixth Assessment Report (IPCC, 2021) stated that the global average temperature for the ten years from 2011 to 2020 is 1.09°C higher than that between 1850 and 1900, primarily due to warming after 2012. Furthermore, they predicted that global warming would increase rainfall intensity and that heavy rains and floods would become more frequent and intense in most parts of Asia. Climate change impacts the soil environment, i.e., soil temperature and water content (Amundson et al., 2015). Changes in the soil temperature and water content can result in shifts in suitable areas for crop cultivation (Sugiura and Yokozawa, 2004), decreased productivity in agriculture and fisheries (Thiault et al., 2019), impacts on soil ecosystems (e.g., Kaneda et al., 2016; Fuentes and Porter, 2013; Onwuka, 2018), and an increase in greenhouse gas emissions due to soil microorganism activity (Schaufler et al., 2010). It is crucial to anticipate future soil temperature and water content to modify crop cultivation practices and improve crop varieties to continue farming in response to climate change.

Some research is already underway to assess the effects of climate change on the soil temperature and water content with simulations of soil water and heat transfers using future climate data. For example, Kato and Nishimura (2015) computed future soil water content at a soybean field in Toyama Prefecture, Japan, using the one-dimensional soil heat and mass transport analysis software HYDRUS-1D (PC-Progress, Prague, Czech Republic) (Šimůnek et al., 2016) in combination with a global circulation model (GCM). The results highlighted a high soil water content frequency, raising the risk of crop wet damage. Using a similar approach, Tsuji et al. (2020) computed soil water content in fields in Yamaguchi Prefecture, Japan. They found that soils are becoming drier in winter

[1]Graduate School of Agricultural and Life Sciences, The University of Tokyo, 1-1-1 Yayoi, Bunkyo-ku, Tokyo 113-8657, Japan.
[2]Department of Civil Engineering, Gifu University, 1-1 Yanagido, Gifu City, Gifu 501-1193, Japan. Corresponding author: Yuki KOJIMA.
[3]Department of Agricultural and Environmental Engineering, Hirosaki University, 3 Bunkyo-cho, Hirosaki City, Aomori 036-8561, Japan.
2024 年 4 月 1 日受稿　2024 年 6 月 22 日受理

and experiencing less drought in summer. Similarly, Asano et al. (2023) assessed climate change's impact on soil temperature and water content in both plains and mountainous regions of Gifu Prefecture, Japan. They found that future change in soil water content is significant in a mountainous region, while future change in soil temperature is remarkable in a plain region. Furthermore, Yoshida et al. (2021) and Slama et al. (2020) investigated the effects of climate change on soil water content and soil salinity levels. Wang et al. (2021) evaluated future soil moisture changes affecting crop growth. Some research focused on forest soils, e.g., Horel et al. (2022) showed an increase in dry days in forests, and Fernandez-Bou et al. (2020) found soil water content change will affect soil CO_2 emissions in the forests.

While several studies have already predicted future soil temperature and water content, there are few, and the targeted areas are limited. This is because information on soil hydraulic properties, such as hydraulic conductivity and water retention curve, and soil thermal properties, such as thermal conductivity and volumetric heat capacity, are necessary when simulating soil temperature and water content. The soil hydraulic and thermal properties are generally determined by sampling soil from the study area and performing a series of laboratory tests. For example, Asano et al. (2023) determined them by the aforementioned processes and additional optimization based on on-site soil monitoring data. However, this determination procedure requires significant time and effort. Predicting future soil temperature and water content would be easier, and the targeted area could be wider if soil hydraulic and thermal properties could be estimated without soil sampling and laboratory tests.

We focused on a method to estimate soil hydraulic and thermal properties from readily available soil information. This estimation method is known as the Pedotransfer function (PTF). The term "PTF" was coined by Bouma (1989) (McBratney et al., 2002). Bouma (1989) developed a method to estimate time-consuming and costly soil hydraulic properties from soil texture and pH. Numerous studies have been conducted on developing PTFs for soil hydraulic properties (e.g., Schaap et al., 1998; Wösten et al., 1999) and thermal properties (e.g., de Vries, 1963; Campbell, 1985). Although the PTFs are convenient, their practicality for evaluating climate change impacts on the soil temperature and water content is unknown. Kato and Nishimura (2017) tested the PTFs to estimate soil hydraulic parameters for soils in Toyama and Fukui cities, Japan, and estimated future soil moisture in agricultural lands. They focused on the hydraulic properties and water content estimation; thus, thermal properties and temperature dynamics in conjunction with the estimation of hydraulic properties and water dynamics were not yet considered.

This study aimed to investigate the utility of estimating soil hydraulic and thermal properties from publicly available soil information, specifically the Japanese Soil Inventory (JSI) (Takata, 2018; NARO, 2021), using multiple estimation approaches. The JSI is a dataset published by the National Agriculture and Food Research Organization (NARO). This dataset contains information on the distribution of soil types and soil information for all of Japan. We compared soil water content, matric potential, and temperature computed with the estimated soil hydraulic and thermal properties to those computed with the properties determined with soil sampling, laboratory tests, and optimization.

2. Materials and Methods

2.1 Study sites

In this study, two experimental sites were selected: the Gifu University experimental field (35° 27' 42.9" N, 136° 44' 21.5" E) (hereafter referred to as Gifu) and the Gifu University Watershed Science Research Center Takayama experimental site (36° 08' 33.0" N, 137° 25' 20.4" E) (hereafter referred to as Takayama). The locations of these sites are shown in Fig. 1. Both field sites are maintained in bare ground conditions. A small amount of litter layer was observed on the ground surface in Takayama. The soil textures of Gifu and Takayama were sandy clay loam and sandy loam. The soil hydraulic and thermal properties values at the study sites were measured by Asano et al. (2023).

2.2 Overview of HYDRUS-1D

This study computed soil temperature and water content using HYDRUS-1D. The HYDRUS-1D expresses one-dimensional vertical liquid water movement in soil using

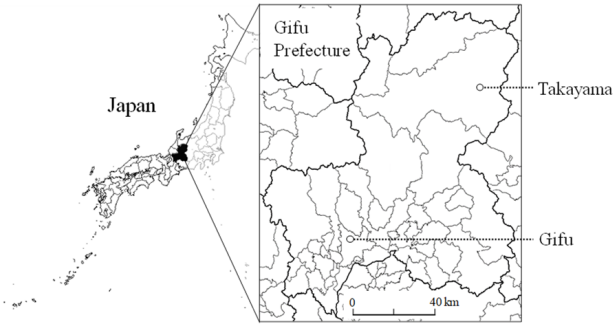


Fig. 1 The locations of the study sites (Gifu and Takayama).

the Richards' equation (Richards, 1931):

$$\frac{\partial \theta}{\partial t} = \frac{\partial}{\partial z}\left[K\left(\frac{\partial h}{\partial z}+1\right)\right] \quad (1)$$

where θ is soil volumetric water content ($m^3\ m^{-3}$), K is hydraulic conductivity ($m\ s^{-1}$), h is soil matric potential (m of water), t is time (s), and z is depth (m). While HYDRUS-1D can consider water vapor movement in the soil, vapor movement is negligible compared to liquid water movement in most cases except for dry conditions, and hence not considered in this study. The relationship between θ and h in unsaturated soils, i.e., water retention curve, is necessary to solve Eq. (1). Although HYDRUS-1D allows the selection of water retention curves from five models, we used the van Genuchten (1980) model (VG model) as:

$$S_e = \frac{\theta-\theta_r}{\theta_s-\theta_r} = (1+|\alpha h|^n)^{-m} \quad (2)$$

where S_e is effective saturation, θ_r and θ_s are residual and saturated volumetric water content ($m^3\ m^{-3}$), respectively, and α is an empirical parameter (m^{-1}). The m and n are dimensionless empirical parameters, and $m = 1 - n^{-1}$. The following equation expresses the K:

$$K = K_s {S_e}^l \left[1-\left(1-{S_e}^{1/m}\right)^m\right]^2 \quad (3)$$

where K_s is saturated hydraulic conductivity ($m\ s^{-1}$), and l is a parameter representing pore connectivity (unitless).

HYDRUS-1D simulates soil temperature based on the heat conduction equation considering convective heat transfer due to liquid water movement:

$$\frac{\partial C_p T}{\partial t} = \frac{\partial}{\partial z}\left(\lambda \frac{\partial T}{\partial z}\right) - C_w q_l \frac{\partial T}{\partial z} \quad (4)$$

where C_p is volumetric heat capacity of soil ($J\ m^{-3}\ °C^{-1}$), T is soil temperature (°C), λ is thermal conductivity ($W\ m^{-1}\ °C^{-1}$), C_w is volumetric heat capacity of liquid water ($J\ m^{-3}\ °C^{-1}$), and q_l is flux density of liquid water ($m\ s^{-1}$). We assumed that heat transfer related to water vapor movement was negligible. The thermal conductivity λ can be selected from the Campbell (1985) model (hereafter, Campbell model) and the Chung and Horton (1987) model (CH model) in HYDRUS-1D. Equation (5) presents the Campbell model for unsaturated soil:

$$\lambda = A + B\theta - (A-F)\exp\left[-(D\theta)^I\right] \quad (5)$$

where A, B, D, F, and I are coefficients. In many mineral soils, A is determined using the dry bulk density ρ_b:

$$A = 0.65 - 0.78\rho_b + 0.60{\rho_b}^2 \quad (6)$$

For mineral soils, B is

$$B = 1.06\rho_b \quad (7)$$

The parameter D represents the water content at which thermal conductivity increases sharply and is highly correlated with clay content. In this case, D is expressed by Eq. (8), where m_c is the volumetric fraction of clay ($m^3\ m^{-3}$).

$$D = 1 + 2.6{m_c}^{-0.5} \quad (8)$$

When the soil particle density is 2.65 $Mg\ m^{-3}$ for mineral soil, F is given by:

$$F = 0.03 + 0.1{\rho_b}^2 \quad (9)$$

The constant I can be set to 4:

$$I = 4 \quad (10)$$

Equation (11) represents the CH model:

$$\lambda = b_1 + b_2\theta + b_3\theta^{0.5} \quad (11)$$

where b_1, b_2, and b_3 are empirical parameters. The CH model is not a PTF; therefore, it is impossible to determine b_1 to b_3 from soil information alone. The procedure to determine them is described in 2.3.4.

The HYDRUS-1D determines surface boundary conditions by solving the surface energy balance based on the input meteorological data (Saito et al., 2006). The surface energy balance can be expressed as follows:

$$R_n - H - LE - G = 0 \quad (12)$$

where R_n is net radiation ($W\ m^{-2}$), H is sensible heat flux ($W\ m^{-2}$), L is latent heat of evaporation ($J\ m^{-3}$), E is evaporation rate ($m\ s^{-1}$), and G is soil heat flux ($W\ m^{-2}$). Precipitation and E from Eq. (12) are used as boundary conditions for water transfer computations, while G is used for heat transfer computations.

2.3 Estimation method of soil hydraulic and thermal properties

The soil hydraulic and thermal properties necessary for HYDRUS-1D simulations were estimated from soil information obtained from JSI. JSI provides nationwide soil distribution and information for different soil classifications. In this study, we acquired information on soil classification, soil carbon content (OC), K_s, and θ values at pF= 0,

1.5, and 2.7. The information available in JSI is for different depths, but we assumed they represent the whole soil profile in this study.

Based on the information, we estimated sand-silt-clay mass ratios (hereafter %SSC), ρ_b, K_s (the K_s value can be obtained from JSI, but we also examined a PTF for K_s), parameters for water retention curve, and parameters for λ models. Estimation was performed using multiple approaches for each parameter, outlined in Sections 2.3.1 to 2.3.4.

2.3.1 Estimation of %SSC

The JSI only provides soil classification (Fig. 2), and exact values of %SSC are difficult to determine. For example, Gifu and Takayama were identified as highly clayey and clayey without specific silt-clay content values. Therefore, we extracted two types of %SSC: the %SSC of each classification's centroid (referred to as Method 1) and the %SSC at the center point of the line that minimizes clay content considered to significantly influence water retention (referred to as Method 2). Fig. 2 includes the %SSC of Method 1 and Method 2 of highly clayey soil as an example. The %SSC determined by Method 1 are 25 % sand, 25 % silt, and 50 % clay corresponding to the center of gravity of the upper triangle. In Method 2, % clay is fixed at 25 % which is the minimum value, and 37.5 % sand and 37.5 % silt correspond to the central of the base of the upper triangle.

2.3.2 Estimation of ρ_b

The ρ_b was estimated with the PTF proposed by Abdelbaki (2018) from *OC* (%). Abdelbaki (2018) investigated various ρ_b estimation approaches and proposed the most suitable one. The optimal estimation formula identified by Abdelbaki (2018) is:

$$\rho_b = (2.684 - 140.943 \times 0.006)\exp(-0.006OC) \quad (13)$$

The *OC* values obtained from JSI were used for Eq. (13).

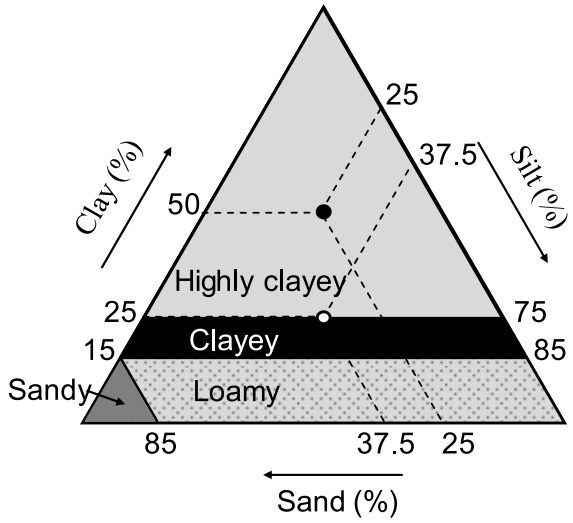


Fig. 2 Triangular diagram of soil classification in the Japanese Soil Inventory. How the percentages of sand, silt, and clay of "highly clayey" soil are determined using Method 1 (center of gravity of the soil texture diagram) and Method 2 (center of line minimizing clay content) is illustrated as an example. Black circles represent Method 1, while white circles represent Method 2.

2.3.3 Estimation of hydraulic property parameters

The three types of K_s values were prepared: i) the value directly obtained from JSI, ii) the value obtained using ROSETTA (Schaap et al., 2001) with the %SSC determined with Method 1 and ρ_b, and iii) the one obtained using ROSETTA with the %SSC determined with Method 2 and ρ_b. The JSI provides a median and variations of K_s. We used the median value. The VG model parameters (θ_s, θ_r, α, n) for the water retention curves were also determined with three approaches: i) by fitting the VG model to the θ values at multiple pF provided by JSI, ii) by estimating with ROSETTA (Schaap et al., 2001) from Method 1-based %SSC and ρ_b, and iii) by estimating with ROSETTA from Method 2-based %SSC and ρ_b. When estimating VG model parameters by fitting to pF-θ data provided by JSI, θ_r and α were fixed at constant values due to the limited number of θ data. The θ_r was fixed at 0.1 $m^3\ m^{-3}$ as soil conditions are assumed never to reach a dry state of 0.1 $m^3\ m^{-3}$. The α values were fixed to 0.01 m^{-1} for Gifu and 0.1 m^{-1} for Takayama, which ensure convergence in HYDRUS-1D computations. Combining the three K_s patterns with the three VG model patterns prepared in a total of nine sets of soil hydraulic properties parameters for each sampling point.

2.3.4 Estimation of thermal property parameters

The λ were estimated with either the Campbell model or Lu et al. (2014) model (hereafter, Lu model) based on the %SSC values obtained from JSI and estimated ρ_b. Equation (14) represents the Lu model:

$$\lambda = \lambda_{dry} + \exp\left(\gamma - \theta^{-\beta}\right) \quad (14)$$

where λ_{dry} is the λ of air-dried samples, and β and γ are shape factors. The λ_{dry} can be estimated with the following equation as revealed by Lu et al. (2007):

$$\lambda_{dry} = -0.56\tau + 0.51 \quad (15)$$

where τ represents soil porosity ($m^3\ m^{-3}$), which can be computed from ρ_b assuming that the soil particle density is 2.65 Mg m^{-3}. The parameters β and γ are determined with the following equations:

$$\beta = 0.67 f_{\mathrm{cl}} + 0.24 \tag{16}$$

$$\gamma = 1.97 f_{\mathrm{sa}} + 1.87 \rho_{\mathrm{b}} - 1.36 f_{\mathrm{sa}} \rho_{\mathrm{b}} - 0.95 \tag{17}$$

where f_{cl} (kg kg^{-1}) and f_{sa} (kg kg^{-1}) are the mass fractions of clay and sand. Since the Lu model is not implemented in HYDRUS-1D, we approximated the Lu model with the CH model and determined the parameters b_1 to b_3 in Eq. (11).

The computation of C_{p} in Eq. (4) in HYDRUS-1D requires the volume fraction of soil solid. We obtained this fraction by dividing ρ_{b} by the particle density (2.65 Mg m^{-3}).

2.4 Determining the optimal estimation approach for soil hydraulic and thermal properties

We computed the soil T, θ, and h from January 1, 2021, to December 31, 2021, using HYDRUS-1D with the soil hydraulic and thermal properties estimated with the approaches mentioned in 2.3. The computation was performed with a 200 cm long homogeneous soil column with a 2 cm node spacing. The initial time step for the simulation was 1×10^{-5} d. Daily meteorological data was used to compute the surface boundary conditions. The bottom boundary conditions were zero pressure head gradient (i.e., free drainage) for water transfer and zero temperature gradient for heat transfer.

Meteorological data necessary for the boundary condition computations were obtained from the NARO Mesh Agricultural Meteorological Data (Ohno et al., 2016; NARO, 2024), created and made publicly available by the NARO. This meteorological data set is a downscaled scenario dataset based on future predictions obtained by providing a warming scenario to GCM, downscaled to 1 km mesh resolution. The NARO Mesh Agricultural Meteorological Data users must select the types of GCM and global warming scenarios. We selected the MIROC5, the GCM developed jointly by the University of Tokyo, the National Institute for Environmental Studies, and the Japan Agency for Marine-Earth Science and Technology for the GCM. The RCP8.5 scenario, the most severe warming scenario within the dataset, was selected. The Meteorological data retrieved from the Mesh Agricultural Meteorological Data for the simulations were daily maximum and minimum air temperatures, daily cumulative precipitation, daily average relative humidity, daily average wind speed, and daily cumulative solar radiation.

Asano et al. (2023) conducted a series of laboratory tests using soil samples collected at the Gifu and Takayama sites and determined parameters for the soil hydraulic and thermal properties through an optimization process based on field observations of soil water content and soil temperature. We also computed the T, θ, and h for the same period using the parameters of Asano et al. (2023). We considered these computations the reference values and compared them with the computations with the parameters determined with JSI and PTFs. The assessment was conducted by calculating the root mean squared error (RMSE) for the soil T, θ, and h values computed with the parameters estimated in this study and with those retrieved from Asano et al. (2023). The estimation approach that provided minimum RMSE was considered optimal for estimating soil hydraulic and thermal properties.

After determining the optimal approach for estimating soil hydraulic and thermal properties estimation, we simulated the future soil T, θ, and h. The computation period was set from 2011 to 2020 as the present and from 2091 to 2100 as the future. Again, we computed T, θ, and h using the parameters retrieved from Asano et al. (2023) and using those estimated with the optimal approach for both the present and future periods. In the case of the optimal approaches for Gifu and Takayama differed, we also performed the same computations by swapping the estimation approach for Gifu and Takayama. Namely, the hydraulic and thermal properties of Gifu were estimated using the optimal approach for Takayama, and vice versa. This examination aimed to determine a more advantageous estimation approach among the two.

HYDRUS-1D can compute temporal changes of T, θ, and h, and the computation results in this study are available every 0.01 d. However, in order to minimize the influence of unusual years such as El Niño events, studies using GCM meteorological data generally average the results of computations over multiple years (e.g., Kato and Nishimura, 2015; Yoshida et al., 2021). Thus, the average of the output values for each month was obtained, and then the average of these values for ten years was computed.

3. Results and Discussion

3.1 Estimated soil hydraulic properties

Table 1 shows the %SSC values extracted from JSI, estimated ρ_{b} values using the Eq. (13), K_{s}, and the VG model parameters. Additionally, values determined by Asano et al. (2023) are also included for comparison. Comparing the obtained parameters with those of Asano et al. (2023), it was found that K_{s} was well estimated using ROSETTA, while JSI tended to overestimate K_{s}. Regarding the VG model, θ_{s} was consistently smaller than Asano et al. (2023) with any estimation approaches, while θ_{r} was larger. The n values were comparable to those reported by Asano et al. (2023). The PTF-based VG parameters repro-

Table 1 The soil texture extracted from the Japanese Soil Inventory (JSI), the estimated dry bulk density, saturated hydraulic conductivity, and van Genuchten (1980) (VG) model parameters for the Gifu and Takayama sites. Experimentally determined parameters retrieved from Asano et al. (2023) were also included.

Site	Soil texture (%)									Dry bulk density (Mg m^{-3})	
	Asano et al. (2023)			Method1 [a)]			Method 2 [a)]			Asano et al. (2023)	Abdelbaki (2018) [b)]
	Sand	Silt	Clay	Sand	Silt	Clay	Sand	Silt	Clay		
Gifu	60	16	24	25	25	50	37.5	37.5	25	1.36	1.39
Takayama	80	9	11	40	40	20	42.5	42.5	15	0.78	1.29

Site	Saturated hydraulic conductivity (m day^{-1})				VG model [d)]			
	Asano et al. (2023)	JSI	ROSETTA (Method 1) [c)]	ROSETTA (Method 2) [c)]	Asano et al. (2023)			
					θ_s (m^3 m^{-3})	θ_r (m^3 m^{-3})	α (m^{-1})	n (-)
Gifu	0.34	1.64	0.12	0.14	0.639	0.057	1.16	1.567
Takayama	6.99	15.55	0.27	0.34	0.894	0.059	1.76	1.605

Site	VG model [d)]											
	JSI data fitting [e)]				ROSETTA (Method 1) [c)]				ROSETTA (Method 2) [c)]			
	θ_s (m^3 m^{-3})	θ_r (m^3 m^{-3})	α (m^{-1})	n (-)	θ_s (m^3 m^{-3})	θ_r (m^3 m^{-3})	α (m^{-1})	n (-)	θ_s (m^3 m^{-3})	θ_r (m^3 m^{-3})	α (m^{-1})	n (-)
Gifu	0.569	0.1	0.01	1.21	0.467	0.127	0.90	1.28	0.416	0.095	0.70	1.39
Takayama	0.625	0.1	0.10	1.24	0.429	0.087	0.70	1.43	0.419	0.078	0.70	1.47

a) "Method 1" and "Method 2" indicate that texture is computed based on the center of gravity of the soil texture diagram and the center of line minimizing clay content, respectively.
b) The bulk density is computed using the equation proposed by Abdelbaki (2018).
c) "ROSETTA" indicates parameters obtained with the software ROSETTA (Schaap et al., 2001) from soil sand, silt, and clay contents.
d) VG model parameters include residual water content (θ_r), saturated water content (θ_s), and empirical parameters (α and n).
e) "JSI data fitting" indicates that the parameters are obtained by fitting the VG model on the volumetric water content-pF values retrieved from JSI.

duced Asano et al. (2023) parameters better in Gifu than in Takayama.

3.2 Optimal estimation approach for soil hydraulic properties

Table 2 shows the RMSE values between the θ and h for 2021 computed using the estimated soil parameters and those computed using Asano et al. (2023) parameters. The RMSE values varied depending on the test site and computation item. In Gifu, K_s and VG model parameters estimated by ROSETTA with Method 2-based %SSC and ρ_b resulted in the minimum RMSE values, which indicates this is the optimal estimation approach for the Gifu site. The RMSE values were 0.0256 m^3 m^{-3} for θ and 0.0018 m for h. While the optimal estimation approaches for both θ and h were the same in Gifu, they varied in Takayama. The combination of K_s published by JSI and VG model parameters determined by fitting the VG model with pF-θ values published by JSI resulted in the minimum RMSE value of 0.0277 m^3 m^{-3} for θ. The combination of K_s published by JSI and VG model parameters determined by ROSETTA with Method 2-based %SSC and ρ_b yielded the minimum RMSE value of 0.2062 m for h. In this study, we put more emphasis on θ and determined that the optimal estimation approach is the one showing the minimum RMSE value of θ. Given that, the optimal estimation approach in Takayama was K_s values published by JSI and VG model determined with the fitting of VG model with pF-θ values. Kato and Nishimura (2017) also showed that the optimal estimation approaches for soil hydraulic properties were not consistent in multiple locations with differing soil textural and cultivation conditions. The same trend was confirmed.

3.3 Estimated soil thermal properties

Table 3 shows the Campbell, Lu, and CH model parameters. The parameters of the CH model determined by Asano et al. (2023) are also included in Table 3. Comparing the CH model parameters estimated with PTF and those presented by Asano et al. (2023), it was observed

Table 2 Root mean square error (RMSE) values of volumetric water contents and matric potentials computed using saturated hydraulic conductivity and van Genuchten (1980) (VG) model parameters extracted from Asano et al. (2023) and estimated. The "Rank" indicates the ascending order of the RMSE.

Estimation Methods		Gifu				Takayama			
Saturated hydraulic conductivity	VG model	Volumetric water content		Matric potential		Volumetric water content		Matric potential	
		RMSE (m^3 m^{-3})	RANK	RMSE (m)	RANK	RMSE (m^3 m^{-3})	RANK	RMSE (m)	RANK
Values published in the JSI	JSI data fitting [b)]	0.1255	7	0.2418	4	**0.0277**	**1**	0.8781	7
Values published in the JSI	Rosetta (Method 1) [a)]	0.0404	3	0.2368	3	0.1839	8	0.2153	2
Values published in the JSI	Rosetta (Method 2) [a)]	0.0491	4	0.3348	6	0.2011	9	**0.2062**	**1**
Rosetta (Method 1) [a)]	JSI data fitting [b)]	0.1831	9	0.5200	9	0.1127	7	1.6314	9
Rosetta (Method 1) [a)]	Rosetta (Method 1) [a)]	0.0844	6	0.3719	7	0.0881	2	0.4742	6
Rosetta (Method 1) [a)]	Rosetta (Method 2) [a)]	0.0273	2	0.2110	2	0.1041	4	0.4612	5
Rosetta (Method 2) [a)]	JSI data fitting [b)]	0.1796	8	0.4826	8	0.1059	5	1.5727	8
Rosetta (Method 2) [a)]	Rosetta (Method 1) [a)]	0.0818	5	0.3342	5	0.0947	3	0.4214	4
Rosetta (Method 2) [a)]	Rosetta (Method 2) [a)]	**0.0256**	**1**	**0.1785**	**1**	0.1110	6	0.4108	3

a) "ROSETTA" indicates parameters obtained with the software ROSETTA (Schaap et al., 2001) from soil sand, silt, and clay contents. "Method 1" and "Method 2" indicate that texture is computed based on the center of gravity of the soil texture diagram and the center of line minimizing clay content, respectively.
b) "JSI data fitting" indicates that the parameters are obtained by fitting the VG model on the volumetric water content-pF values retrieved from JSI.

Table 3 Estimated thermal conductivity model parameters for the Campbell (1985) model, Lu et al. (2014) model, and Chung and Horton (1987) model. Experimentally determined parameters for Chung and Horton (1987) model retrieved from Asano et al. (2023) were also included.

Site	Campbell (1985) model								Lu te al. (2014) model					
	Method 1 [a)]				Method 2 [a)]				Method 1 [a)]			Method 2 [a)]		
	A	B	D	E	A	B	D	E	λ_{dry}	β	γ	λ_{dry}	β	γ
Gifu	1.566	1.470	0.397	6.814	1.680	1.470	0.397	7.713	0.244	0.408	1.671	0.244	0.491	1.681
Takayama	1.587	1.366	0.371	6.814	1.608	1.366	0.371	7.713	0.223	0.508	1.552	0.223	0.525	1.558

Site	Chung and Horton (1987) model [b)]								
	Method 1 [a)]			Method 2 [a)]			Asano et al. (2023)		
	b_1	b_2	b_3	b_1	b_2	b_3	b_1	b_2	b_3
Gifu	0.000	0.128	2.222	0.000	2.281	0.370	0.092	0.100	1.752
Takayama	0.000	1.020	1.165	0.062	2.073	0.207	1.037	4.620	−4.372

a) "Method 1" and "Method 2" indicate that texture is computed based on the center of gravity of the soil texture diagram and the center of line minimizing clay content, respectively.
b) The parameters with Method 1 and Method 2 were obtained by the fitting of Chung and Horton (1987) model on the thermal conductivity curves estimated with the Lu et al. (2014) model.

that the estimated parameters of the Gifu site were close to the parameters of Asano et al. (2023), while parameters of the Takayama site were not. This difference may be attributed to the high organic content in the forest soils of Takayama. There was no significant difference between Method 1 and Method 2.

3.4 Optimal estimation approach for soil thermal properties

Table 4 shows the RMSE values between T computed with the thermal properties estimated with PTF and T computed with those presented by Asano et al. (2023), which is treated as a reference. The results indicate that T simu-

Table 4 Root mean square error (RMSE) values of temperature computed using parameters retrieved from Asano et al. (2023) and estimated in Gifu and Takayama. The "Rank" indicates the ascending order of the RMSE.

Estimation methods of thermal conductivity	Gifu		Takayama	
	RMSE (°C)	RANK	RMSE (°C)	RANK
Campbell (1985)model (Method 1) [a)]	0.5555	3	3.2598	3
Campbell (1985)model (Method 2) [a)]	0.6032	4	3.5355	4
Lu et al. (2014) (Method 1) [a),b)]	**0.4613**	**1**	3.0201	2
Lu et al. (2014) (Method 2) [a),b)]	0.4708	2	**2.9073**	**1**

a) "Method 1" and "Method 2" indicate that texture is computed based on the center of gravity of the soil texture diagram and the center of line minimizing clay content, respectively.
b) Because the Lu et al. (2014) model was not implemented in HYDRUS-1D, Chung and Horton (1987) model fitted on the thermal conductivity curves estimated with Lu et al. (2014) was used for the simulations.

Table 5 Optimal estimation approaches for soil hydraulic and thermal properties in Gifu and Takayama.

Site	Parameters	Optimal estimation method
Gifu	Saturated hydraulic conductivity	ROSEETA (Method 2) [b)]
	Water retention curve [a)]	ROSETTA (Method 2) [b)]
	Thermal conductivity	Lu et al. (2014) model (Method 1) [b),c)]
Takayama	Saturated hydraulic conductivity	Values published in the Japanese Soil Inventory (JSI)
	Water retention curve [a)]	JSI data fitting [d)]
	Thermal conductivity	Lu et al. (2014) model (Method 2) [b),c)]

a) van Genuchten (1980) model parameters.
b) "Method 1" and "Method 2" indicate that texture is computed based on the center of gravity of the soil texture diagram and the center of line minimizing clay content, respectively.
c) Because the Lu et al. (2014) model was not implemented in HYDRUS-1D, Chung and Horton (1987) model fitted on the thermal conductivity curves estimated with Lu et al. (2014) was used for the simulations.
d) "JSI data fitting" indicates that the parameters are obtained by fitting the VG model on the volumetric water content-pF values retrieved from JSI.

lated with the Lu model (approximated by the CH model) better fits the reference values than the Campbell model in both Gifu and Takayama. In Gifu, Lu model parameters estimated from Method 1-based %SSC were optimal, with an RMSE value of 0.4613°C. The RMSE value was slightly higher with Method 2-based %SSC (0.4708°C), indicating a minor influence of the %SSC determination from JSI information. There was also no significant difference in RMSE values due to the difference in %SSC determination for Takayama. The Method 2-based %SSC resulted in a slightly lower RMSE of 2.9073°C compared to 3.0201°C with Method 1-based %SSC. Simulations of Gifu showed better agreement with the reference values than simulations of Takayama.

3.5 Estimation of future soil temperature, water content, and matric potential with the optimal parameters

Table 5 summarizes the optimal estimation approaches for soil hydraulic and thermal properties parameters. They include the K_s estimated with ROSETTA from Method 2-based %SSC and ρ_b, VG model parameters estimated with the same, and the λ estimated with the Lu model from Method 1-based %SSC for Gifu. For Takayama, they include the K_s retrieved from JSI, VG model parameters determined by fitting with pF-θ values published by JSI, and λ estimated with the Lu model from Method 2-based %SSC. Evaluations of the future soil T, θ, and h were performed with the optimally determined parameters.

Fig. 3 shows the present (average from 2011 to 2020) and future (average from 2091 to 2100) soil T, θ, and h at a depth of 20 cm. The figure displays computations with the optimal estimation approaches (Table 5) and those with parameters from Asano et al. (2023), which is considered as a reference. While the T computed with estimated parameters and the reference values agreed well both in the present and future in Gifu (Fig. 3(a)), they differed in Takayama approximately 3°C throughout the year both in the present and future (Fig. 3(b)). The simulated θ and reference values of Gifu (Fig. 3(c)) showed minor differences from January to March and in December, both in the present and future. However, relatively large differences were observed in other months, with a maximum difference of about 0.02 $m^3\ m^{-3}$ in August in the future. The simulated θ and reference values of Takayama (Fig. 3(d)) showed more sig-

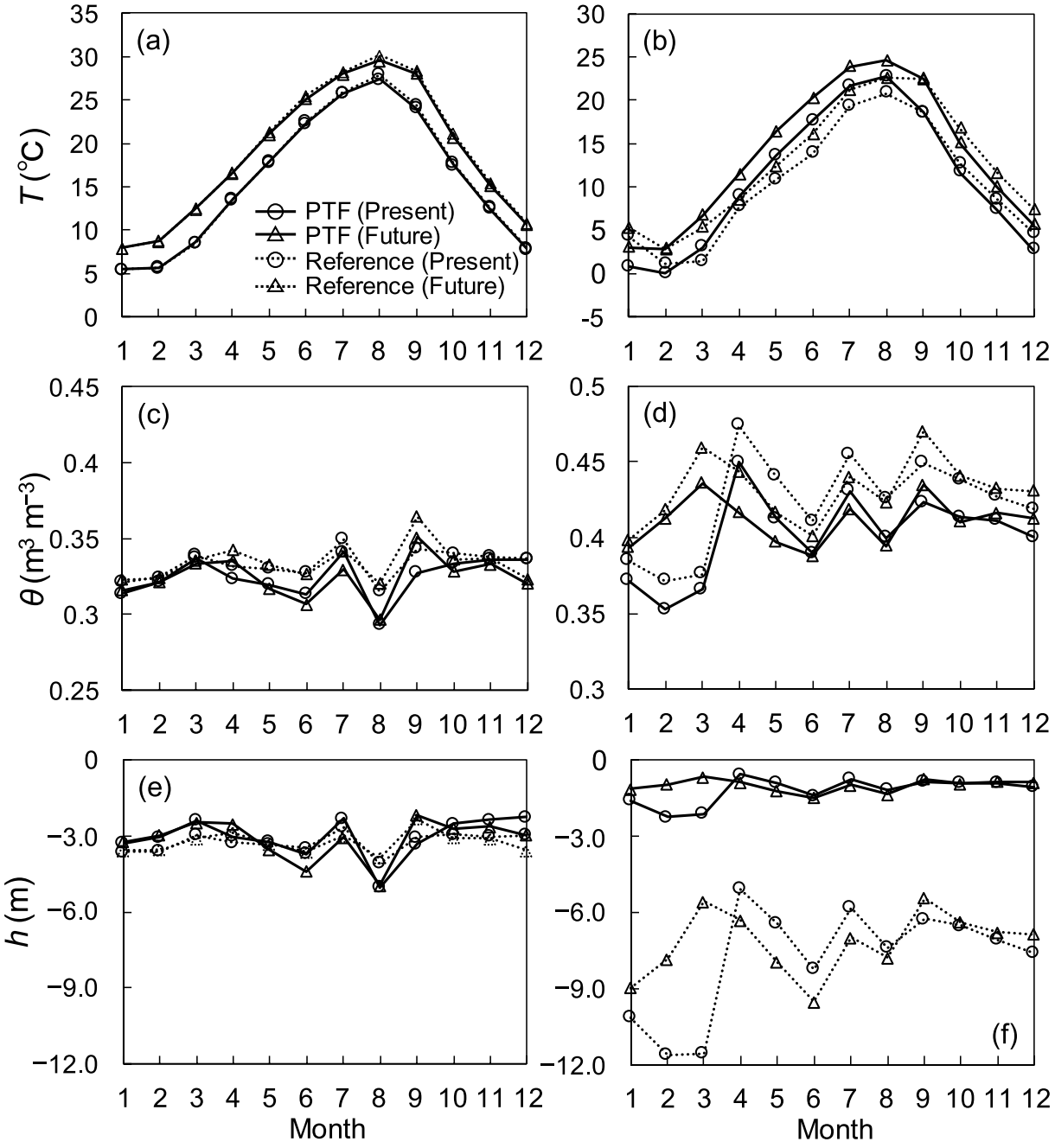


Fig. 3 The soil temperature (T), volumetric water content (θ), and matric potential (h) at 20 cm depth in Gifu and Takayama. Each panel shows (a) T in Gifu, (b) T in Takayama, (c) θ in Gifu, (d) θ in Takayama, (e) h in Gifu, and (f) h in Takayama. The "PTF" indicates the computations with soil hydraulic and thermal properties estimated with pedtransfer functions and the Japanese Soil Inventory, and "Reference" indicates the computations with soil hydraulic and thermal properties retrieved from Asano et al. (2023). The "Present" and "Future" include the computations for 2011–2020 and for 2091–2100, respectively.

nificant differences than those in Gifu, both in the present and future. The difference in θ persisted at around 0.02 m^3 m^{-3} from June to December. The simulated h of Gifu (Fig. 3(e)) with estimated parameters and the reference values were consistent. The differences in future change due to the estimated parameter were at most 0.5 m. The simulated h of Takayama (Fig. 3(f)) showed differences in both present and future computations associated with the estimated parameters. Differences were particularly significant from January to March in the present, showing an average difference of 9 m. The difference decreases after April but is still 6 m on average. The considerable difference in h can be attributed to the slight differences in water retention curves, which results in large variation in h even when θ value is similar.

The future prediction of soil T, θ, and h with the soil

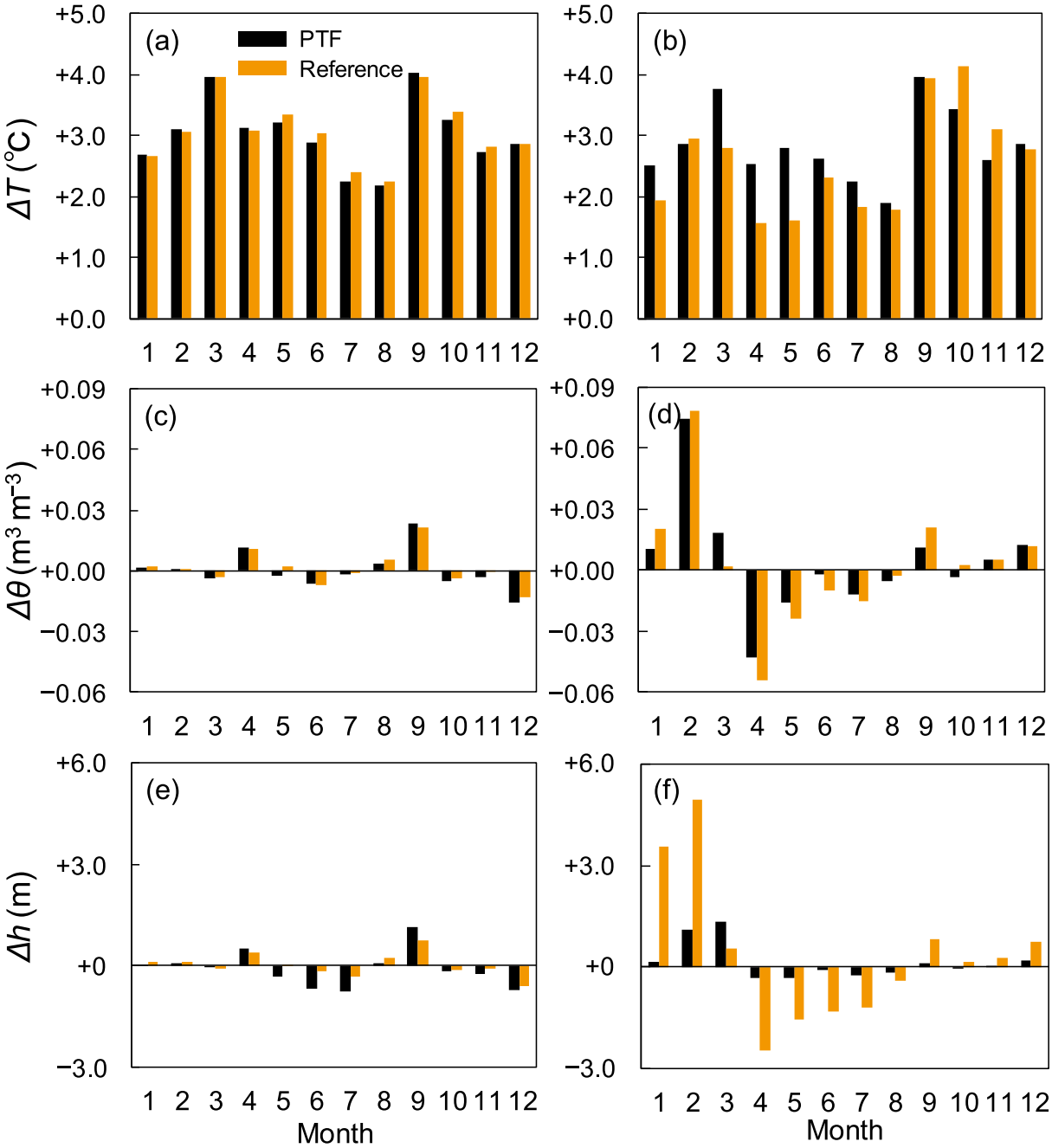


Fig. 4 The computed future change in soil temperature (ΔT), in volumetric water content ($\Delta\theta$), and in matric potential (Δh) at 20 cm depth. Each panel shows (a) ΔT in Gifu, (b) ΔT in Takayama, (c) $\Delta\theta$ in Gifu, (d) $\Delta\theta$ in Takayama, (e)Δh in Gifu, and (f) Δh in Takayama. The "PTF" indicates the computations with soil hydraulic and thermal properties estimated with pedtransfer functions and the Japanese Soil Inventory, and "Reference" indicates the computations with soil hydraulic and thermal properties retrieved from Asano et al. (2023).

hydraulic and thermal properties parameters from Asano et al. (2023) was accurately reproduced with the estimated soil hydraulic and thermal properties only for T at the Gifu site; however, T at the Takayama site as well as θ and h at both locations were not adequately reproduced. This may be attributed to the PTF reproducibility of the actual soil hydraulic and thermal properties. Thus, we focused on the future change of soil T, θ, and h, i.e., ΔT, $\Delta\theta$, and Δh, which represent the differences between present and future values. Fig. 4 illustrates ΔT, $\Delta\theta$, and Δh in Gifu and Takayama. The ΔT computed with parameters from Asano et al. (2023) and those computed with the estimated parameters were consistent in Gifu. The same trend was found in Takayama, while slight differences were observed from March to May, with a maximum difference of 1.18°C (Fig. 4(a, b)). Similarly, $\Delta\theta$ (Fig. 4(c, d)) showed minor differences with a maximum difference of 0.0055 m^3 m^{-3} in Gifu and 0.0084 m^3 m^{-3} in Takayama. It is an important finding that the ΔT and $\Delta\theta$ can be accurately determined with the estimated soil hydraulic and thermal properties.

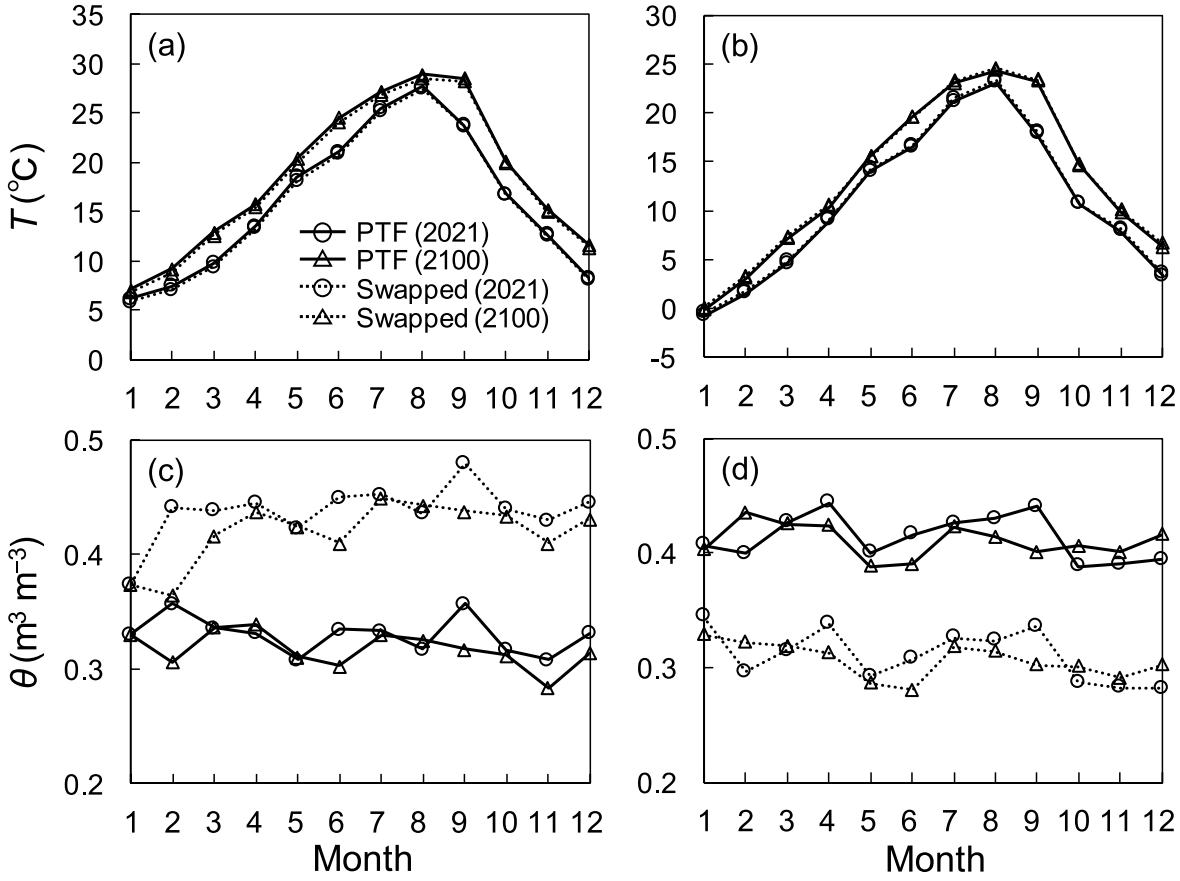


Fig. 5 The computed soil temperature (T) and volumetric water content (θ) at 20 cm depth in Gifu and Takayama. Each panel shows (a) T in Gifu, (b) T in Takayama, (c) θ in Gifu, and (d) θ in Takayama. The "PTF" indicates the computations with soil hydraulic and thermal properties estimated with the optimal estimation approaches for each site, and "Swapped" indicates the computations with the soil hydraulic and thermal properties estimated with the swapped optimal estimation approaches for the two sites.

The Δh (Fig. 4 (e, f)) showed a relatively large difference of up to 4.5 m (in Takayama in February). The possible reasons might be the optimal estimation approaches for the VG model were determined based on θ rather than h, and a small variation of the water retention curve can cause a large difference in h. The Δh was difficult to simulate with the estimated soil hydraulic and thermal properties accurately.

It was found that using estimated soil hydraulic and thermal properties in the future prediction of soil T, θ does not pose any significant issues if we focus on future changes amount. However, the optimal estimation approaches for soil hydraulic and thermal properties differ between Gifu and Takayama. This fact may indicate that the optimal estimation approach varies depending on the location, which is undesirable. Thus, we performed the simulation by swapping the optimal estimation approach described in 2.4. Fig. 5 shows the computed T, θ at a depth of 20 cm by swapping the optimal estimation approach. Fig. 5 only shows the results of 2021 and 2100 since other years showed similar trends. The T exhibited similar values regardless of the parameter estimation approach in both Gifu and Takayama (Fig. 5 (a, b)). Thus, the parameter estimation approach may not be crucial for predicting future changes in T. Swapping the estimation approach resulted in the overestimation of θ in Gifu (Fig. 5 (c)); conversely, θ was underestimated by the swapping in Takayama (Fig. 5 (d)). The estimation method of λ was changed from Rank 1 to Rank 2 in both Gifu and Takayama (Table 4) due to parameter swapping, so it was a relatively good-fit estimation method even after the swapping. The estimation method for θ was replaced by the method from Rank 1 to Rank 7 in Gifu and from Rank 1 to Rank 6 in Takayama (Table 2), resulting in low-fitting methods. These factors may have affected the results. Here, we also checked the future change quantity $\Delta\theta$ (Fig. 6). It was observed that the differences in $\Delta\theta$ due to the swapping of the parameter estimation approach were minor in both Gifu and Takayama. The maximum difference in Gifu was 0.025 m^3 m^{-3} in February, while the maximum difference in Takayama was 0.010 m^3 m^{-3} in February. It was concluded that the estimation approach for hydraulic property parameters is also not as crucial for

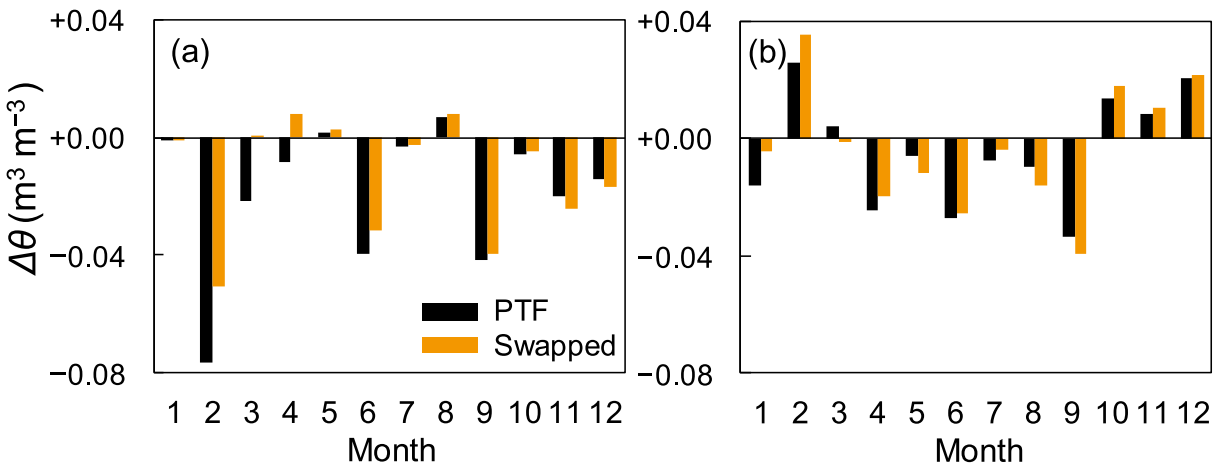


Fig. 6 The future change in volumetric water content ($\Delta\theta$) at 20 cm depth in (a) Gifu and (b) Takayama. The "PTF" indicates the computations with soil hydraulic and thermal properties estimated with the optimal estimation approaches for each site, and "Swapped" indicates the computations with the soil hydraulic and thermal properties estimated with the swapped optimal estimation approaches for the two sites.

predicting $\Delta\theta$, i.e., either of the easier approaches can be selected.

4. Conclusions

This study investigated the utility of estimating soil hydraulic and thermal properties from publicly available soil information using multiple estimation approaches. We retrieved soil information from JSI and used PTFs to estimate the soil hydraulic and thermal properties. Soil T, θ, and h were computed using the estimated parameters, and the results were compared with the computations based on the parameters provided by the literature. There were errors in the T, θ and h due to the estimated parameters, while the results in Gifu were better than those in Takayama. When the future change amounts from present to future are focused, no considerable error was observed in both sites. This result suggests that focusing on future change amounts may eliminate the enormous effort of collecting soil samples from the study area and performing laboratory tests when determining soil hydraulic and thermal properties. Focusing on future change amounts may also eliminate the need to use different estimation approaches of the soil hydraulic and thermal properties for various locations. Although validation at other locations and under different surface conditions is needed, these facts are valuable for future studies on the effects of climate change on the soil T, θ at various sites.

Acknowledgments

This work was supported by Grants-in-Aid for Early Career Scientist 21K14940 from the Japan Society for the Promotion of Science, Ogawa Science and Technology Foundation research grants, and the Joint Usage/Research Grant of the River Basin Research Center (2021-G-009), Gifu University. The data used in this study were obtained from the "Japanese Soil Inventory (NARO, National Agriculture and Food Research Organization)" and "The Agro-Meteorological Grid Square Data (NARO, National Agriculture and Food Research Organization)."

References

Abdelbaki, A.M. (2018): Evaluation of pedotransfer functions for predicting soil bulk density for U.S. soils. Ain Shams Engineering Journal, 9: 1611–1619.

Amundson, R., Berhe, A.A., Hopmans, J.W., Olson, C., Sztein, A.E. and Sparks, D.L. (2015): Soil science: Soil and human security in the 21st century. Science, 348(6235): 1261071.

Asano, J., Kojima, Y., Kato, C. and Kamiya, K. (2023): Climate change impacts on soil moisture and temperature in the plain and mountainous regions of Gifu prefecture, Japan. IOP Conf. Ser., Earth Environ. Sci., 1165: 012045.

Bouma, J. (1989): Using soil survey data for quantitative land evaluation. In B.A. Stewart (Eds.), Advances in soil science, Volume 9, pp. 177–213. Springer-Verlag.

Campbell, G.S. (1985): Soil physics with basic — transport models for soil-plant systems. Elsevier. New York.

Chung, S.O. and Horton, R. (1987): Soil heat and water flow with a partial surface mulch. Water Resour. Res., 223(12): 2175–2186.

de Vries, D.A. (1963): Thermal properties of soils. In van Wijk, W.R. (ed.) Physics of plant environment, 2nd edi-

tion, pp. 210–235. North Holland Publ., Amsterdam.

Fernandez-Bou, A.S., Dierick, D., Allen, M.F. and Harmon, T.C. (2020): Precipitation-drainage cycles lead to hot moments in soil carbon dioxide dynamics in a Neotropical wet forest. Global Change Biol., 26: 5303–5319.

Fuentes, M.M.P.B. and Porter, W.P. (2013): Using a microclimate model to evaluate impacts of climate change on sea turtles. Ecol. Model., 251: 150–157.

Horel, Á., Zsigmond, T., Farkas, C., Gelybó, G., Tóth, E., Kern, A. and Bakacsi, Z. (2022): Climate change alters soil water dynamics under different land use types. Sustainability, 14(7): 3908.

IPCC (2021): Climate Change 2021: The physical science basis. Contribution of working group I to the sixth assessment report of the intergovernmental panel on climate change. Cambridge University Press, Cambridge.

Kaneda, S., Ohkubo, S., Wagai, R. and Yagasaki, Y. (2016): Soil temperature and moisture-based estimation of rates of soil aggregate formation by the endogeic earthworm Eisenia japonica (Michaelsen, 1892). Biol Fertil Soils, 52: 789–797.

Kato, C. and Nishimura, T. (2015): Temporal downscaling methods of GCM projections for predicting soil moisture in agricultural land (in Japanese with English abstract). Irrigation, Drainage and Rural Engineering Journal, 295: 11–19.

Kato, C. and Nishimura, T. (2017): Predicting soil moisture condition in arbitrary agricultural lands using the digital soil map and soil physical properties database. Paddy Water Environ., 15: 159–169.

Lu, S., Gong, T.S. and Horton, R. (2007): An improved model for predicting soil thermal conductivity from water content. Soil Sci. Soc. Am. J., 71(1): 8–14.

Lu, Y., Lu, S., Horton, R. and Ren, T. (2014): An empirical model for estimating soil thermal conductivity from texture, water content, and bulk density. Soil Sci. Soc. Am. J., 78(6): 1859–1868.

McBratny, A.B., Minasny, B., Cattle, S.R. and Vervoort, R.W. (2002): From pedotransfer functions to soil inference systems. Geoderma, 109: 41–73.

NARO (2021): Japanese Soil Inventory (in Japanese). Available at https://soil-inventory.rad.naro.go.jp/. (2024. 5. 3)

NARO (2024): NARO Mesh Agricultural Meteorological Data (in Japanese). Available at https://amu.rd.naro.go.jp/. (2024. 5. 3)

Ohno, H., Sasaki, K., Ohara, G. and Nakazono, K. (2016): Development of grid square air temperature and precipitation data compiled observed, forecasted, and climatic normal data (in Japanese with English abstract). Climate in Biosphere, 16: 71–79.

Onwuka, B.M. (2018): Effects of soil temperature on some soil properties and plant growth. Adv Plants Agric Rec., 8(1): 34–37.

Richards, L.A. (1931): Capillary conduction of liquids through porous mediums. PHYSICS, 1: 318–333.

Saito, H., Šimůnek, J. and Mohanty, B.P. (2006): Numerical analysis of coupled water, vapor, and heat transport in the vadose zone. Vadose Zone J., 5(2): 784–800.

Schaap, M. G., Leij, F. J. and van Genuchten, M.Th. (1998): Neural network analysis for hierarchical prediction of soil hydraulic properties. Soil Sci. Soc. Am. J., 62(4): 847–855.

Schaap, M.G., Leij, F.J. and van Genuchten, M.Th. (2001): ROSETTA: a computer program for estimating soil hydraulic parameters with hierarchical pedotransfer functions. J. Hydrol., 251: 163–176.

Schaufler, G., Kitzler, B., Schindlbacher, A., Skiba, U., Sutton, M.A. and Zechmeister-Boltenstern, S. (2010): Greenhouse gas emissions from European soils under different land use: effects of soil moisture and temperature. Eur. J. Soil Sci., 61: 683–696.

Šimůnek, J., van Genuchten, M.Th. and Šejna, M. (2016): Recent developments and applications of the HYDRUS computer software packages. Vadose Zone J., 15(7): 1–25.

Slama, F., Gargouri-Ellouze, E. and Bouhlila, R. (2020): Impact of rainfall structure and climate change on soil and groundwater salinization. Climatic Change, 163: 395–413.

Sugiura, T. and Yokozawa, M. (2004): Impact of global warming on environments for apple and satsuma mandarin production estimated from changes of the annual mean temperature (in Japanese with English abstract). Journal of the Japanese Society for Horticultural Science, 73(1): 72–78.

Takata, Y. (2018): Development of Japanese Soil Inventory and its utilization for sustainable soil management (in Japanese). JATAFF Journal, 6(11): 7–12.

Thiault, L., Mora, C., Cinner, J.E., Cheung, W.W.L., Graham, N.A.J., Januchowski-Hartley, F.A., Mouillot, D., Sumaila, U.R. and Claudet, J. (2019): Escaping the perfect storm of simultaneous climate change impacts on agriculture and marine fisheries. Science Advances, 5: 1–9.

Tsuji, T., Fujii, T. and Sakaguchi, A. (2020): Future prediction of field soil moisture using ELPIS-JP (in Japanese with English abstract). Journal of the Japanese Society of Soil Physics, 145: 3–10.

van Genuchten, M.Th. (1980): A closed-form equation for predicting the hydraulic conductivity of unsaturated soils. Soil Sci. Soc. Am. J., 44(5): 892–898.

Wang, X., Li, Y., Chen, X., Wang, H., Li, L., Yao N., Liu, D.L., Biswas, A. and Sun, S. (2021): Projection of the climate change effects on soil water dynamics of summer maize grown in water repellent soils using APSIM and HYDRUS-1D models. Computers and Electronics in Agriculture, 185: 106142.

Wösten, J.H.M., Lilly, A., Nemes, A. and Le Bas, C. (1999): Development and use of a database of hydraulic properties of European soils. Geoderma, 90: 169–185.

Yoshida, K., Sritumboon, S., Srisutham, M., Homma, K., Maki, M. and Oki, K. (2021): Climate change impact on soil salt accumulation in Khon Kaen, Northeast Thailand. Hydrological Research Letters, 15(4): 92–97.

This article is an open access article under the terms of the Creative Commons Attribution (CC BY) license (https://creativecommons.org/licenses/by/4.0/).

要　　旨

土壌水分量，地温の将来予測計算に必要な土壌水理特性，土壌熱特性の決定は，多くの時間と労力，費用を要する．本研究では，公開された土壌情報とペドトランスファー関数（PTF）を用いた土壌水理・熱特性推定法の有用性を検討した．土壌情報を日本土壌インベントリーから抽出し，複数の PTF で土壌水理・熱特性を推定した．推定した土壌水理・熱特性と既往研究から得た土壌水理・熱特性を用いて土壌環境を計算し，両者の誤差が最小となる推定手法を最適とした．その後，最適推定手法で得た土壌水理・熱特性を用いて将来土壌環境を計算し，既往研究の計算結果と比較した．その結果，地温や体積含水率の予測結果では両者の間で差が生じたが，現在から将来までの変化量では大差はなかった．将来変化量評価に限定すれば，公開された土壌情報と PTF によって土壌水理・熱特性を推定しても妥当な評価が可能であることがわかった．

キーワード：ペドトランスファー関数，土壌水理特性，土壌熱特性，気候変動，HYDRUS-1D